

ORIGINAL ARTICLE

# Protective Effects of Neural Crest-Derived Stem Cell-Conditioned Media against Ischemia-Reperfusion-Induced Lung Injury in Rats

Chung-Kan Peng,<sup>1</sup> Shu-Yu Wu,<sup>2</sup> Shih-En Tang,<sup>1</sup> Min-Hui Li,<sup>3</sup> Shih-Shiuan Lin,<sup>2</sup> Shi-Jye Chu,<sup>4,5,6</sup> and Kun-Lun Huang<sup>1,2,5,6</sup>

**Abstract**—Current treatments for ischemia-reperfusion (IR)-induced acute lung injury are limited. Mesenchymal stem cell-conditioned medium (CM) has been reported to attenuate lung injury. Neural crest stem cells (NCSCs), a type of multipotent stem cells, are more easily obtained than mesenchymal stem cells. We hypothesize that NCSC-CM has anti-inflammatory properties that could protect against IR-induced lung injury in rats. In this study, NCSC-CM was derived from rat NCSCs. Typical acute lung injury was induced by 30-min ischemia followed by 90-min reperfusion in adult male Sprague–Dawley rats. Bronchoalveolar lavage fluid (BALF) and lung tissues were collected to analyze the degree of lung injury after the experiment. NCSC-CM was administered before ischemia and after reperfusion. NCSC-CM treatment significantly attenuated IR-induced lung edema, as indicated by decreases in pulmonary vascular permeability, lung weight gain, wet to dry weight ratio, lung weight to body weight ratio, pulmonary arterial pressure, and protein level in BALF. The levels of tumor necrosis factor- $\alpha$  and interleukin-6 in the BALF were also significantly decreased. Additionally, NCSC-CM improved lung pathology and neutrophil infiltration in the lung tissue, and significantly suppressed nuclear factor (NF)- $\kappa$ B activity and I $\kappa$ B- $\alpha$  degradation in the lung. However, heating NCSC-CM eliminated these protective effects. Our experiment demonstrates that NCSC-CM treatment decreases IR-induced acute lung injury and that the protective mechanism may be attributable to the inhibition of NF- $\kappa$ B activation and the inflammatory response. Therefore, NCSC-CM may be a novel approach for treating IR-induced lung injury.

**KEY WORDS:** acute lung injury; ischemia-reperfusion; neural crest stem cell; conditioned media.

<sup>1</sup> Division of Pulmonary and Critical Care Medicine, Department of Internal Medicine, Tri-Service General Hospital, National Defense Medical Center, Taipei, Taiwan

<sup>2</sup> Institute of Aerospace and Undersea Medicine, National Defense Medical Center, Taipei, Taiwan

<sup>3</sup> Department of Physical Medicine and Rehabilitation, Kaohsiung Veterans General Hospital, Kaohsiung, Taiwan

<sup>4</sup> Division of Rheumatology, Immunology and Allergy, Department of Internal Medicine, Tri-Service General Hospital, National Defense Medical Center, Taipei, Taiwan

<sup>5</sup> Institute of Aerospace and Undersea Medicine, National Defense Medical Center, 161 Ming-Chuan East Road, Section 6, Neihu 114, Taipei, Taiwan, Republic of China

<sup>6</sup> To whom correspondence should be addressed at Institute of Aerospace and Undersea Medicine, National Defense Medical Center, 161 Ming-Chuan East Road, Section 6, Neihu 114, Taipei, Taiwan, Republic of China. E-mails: dl204812@mail.ndmctsg.edu.tw; kun@mail.ndmctsg.edu.tw

## INTRODUCTION

Despite advances in intensive care, the morbidity and mortality of acute lung injury and acute respiratory distress syndrome (ALI/ARDS) remain high. Thus, it is imperative to discover innovative therapies to improve the treatment of this severe illness [1]. Recent experimental studies have suggested that allogeneic mesenchymal stem cells (MSC) have therapeutic potential in multiple preclinical injury models, such as myocardial infarction, diabetes, sepsis, graft-versus-host disease, inflammatory bowel disease, hepatic failure, and acute renal failure [2]. Furthermore, MSC therapy has been investigated in various animal models of ALI/ARDS. These studies have shown the beneficial

effects of MSCs in ALI/ARDS induced by bleomycin, ischemia-reperfusion (IR), live *Escherichia coli* bacteria, ventilator, lipopolysaccharides (LPS), and cecal ligation and puncture [2–4]. Based on these preclinical studies, MSCs were suggested to reduce the severity of lung injury as well as enhance repair.

Originally, the protective mechanisms of MSCs were thought to occur through cell engraftment in the lung, which would repair the endothelial/epithelial cells or result in MSC differentiation into specific lung cell types. However, many subsequent *in vivo* studies demonstrated low engraftment rates (<1%) in lung injury models [2]. Additionally, the protective effect of MSCs was found to be comparable to MSC-conditioned medium (CM) alone [5]. Therefore, the beneficial effects of MSCs appear to be a result of the release of various paracrine factors with immunomodulatory properties. The use of MSC-CM has several advantages: MSC-CM can be easily generated, frozen, and transported, does not contain live cells, and cannot be rejected by the host immune system. Thus, the administration of MSC-CM may offer a new approach for the treatment of ALI/ARDS.

In addition to the bone marrow, other sources of MSCs have been studied [6]. Neural crest stem cells (NCSCs) are multipotent stem cells derived from the embryonic neural crest found in several embryonic and adult locations [7]. Particularly, multipotent NCSCs are also present in the hair follicle bulge and are easily acquired without ethical concerns [7]. In the present study, we investigated the potential therapeutic effects of NCSC-CM in a rat model of IR-induced acute lung injury.

## MATERIALS AND METHODS

### Animals and Housing Conditions

Male Sprague–Dawley rats weighing  $350 \pm 20$  g were purchased from BioLASCO Taiwan Co., Ltd. (Taipei, Taiwan). All experiments were approved by the Animal Review Committee at the National Defense Medical Center (Taipei, Taiwan) and conducted in accordance with the guidelines of the National Institutes of Health (National Academy Press 1996).

### Isolation and Culture of Rat NCSCs

We prepared hair follicle bulges from the adult Sprague–Dawley rats as previously described [8]. Briefly, whisker follicles were obtained from the whisker pads of male Sprague–Dawley rats. The collagen capsule and

dermal sheath of the end bulbs were microdissected, and the follicular papilla was exposed using fine forceps under a binocular microscope (Nikon SMZ100; Nikon, Tokyo, Japan). The dissected follicular papillae were placed in 35-mm petri dishes containing RPMI-1640 medium (Invitrogen, Carlsbad, CA, USA) supplemented with 15% heat-inactivated fetal bovine serum (HyClone, Logan, UT, USA), 10 units/mL penicillin, and 10  $\mu$ g/mL streptomycin (Invitrogen), and incubated at 37 °C in a 5% CO<sub>2</sub> humidified incubator for 5 days. The culture medium was replaced every 3 days, and the dermal papilla cells were sub-cultured when they reached 80% confluence. The dermal papilla cells used for this experiment were passaged 10 to 15 times.

### Immunophenotype Characterization of NCSCs

Ten days after isolation and culture, the cells were passaged and plated on collagen-coated cover slips overnight, washed in PBS and fixed in 4% paraformaldehyde for 10 min. The fixed cells were washed in PBS and incubated in blocking buffer containing 10% goat serum (Sigma-Aldrich, St. Louis, MO, USA) and 0.3% Triton X-100 (Fluka, St. Louis, MO, USA) at room temperature for 30 min. Cells were then incubated at 4 °C overnight with one of the following primary antibodies: anti-SOX10 (1:200, rabbit polyclonal IgG; Abcam, Cambridge, MA, USA), anti-Snail 1 (1:100, rabbit polyclonal IgG; Santa Cruz, Biotechnology, Inc., Santa Cruz, CA, USA), or anti-p75 (1:400, rabbit polyclonal IgG; Abcam). The next day, the cells were rinsed three times to remove the unbound primary antibodies and then incubated at room temperature for 2 h with secondary antibody (Alexa Fluor 555-conjugated goat anti-rabbit, 1:400; Invitrogen). The cell nuclei were counterstained with 4',6-diamidino-2-phenylindole (DAPI, 1  $\mu$ g/mL; Invitrogen) in PBS, in the dark and at room temperature for 1 min. After washing, the stained cover slips were removed, mounted on a slide with mounting media, and visualized using a fluorescence microscope (LeicaDM2500; Leica Microsystems GmbH, Wetzlar, Germany) equipped with an EMCCD camera (LucaEM R DL-604M; Andor Technology, Belfast, UK).

### NCSC-CM Preparation

To prepare the CM, the NCSCs ( $5 \times 10^6$ ) were seeded in a 60-mm culture dish. The NCSCs were incubated with serum-free Dulbecco's modified Eagle's medium (DMEM, Sigma-Aldrich) for 24 h to produce CM. The CM was collected and filtered through a 0.2- $\mu$ m filter to remove cellular debris. The adherent cells were trypsinized, stained

with trypan blue, and counted. The medium obtained from  $5 \times 10^6$  cells yielded 15 mL of primary CM, which was further desalted and concentrated approximately 25-fold, using ultrafiltration units with a 3-kDa molecular weight cutoff (Amicon Ultra-PL 3; Millipore, Billerica, MA, USA), yielding a final volume of 600  $\mu$ L CM [9]. Serum-free DMEM, desalted and concentrated 25-fold, served as the vehicle control [9].

### Isolated and Perfused Lung Model

The preparation of isolated rat lungs *in situ* was performed as previously described [10, 11]. Briefly, rats were anesthetized with intraperitoneal sodium pentobarbital (50 mg  $\text{kg}^{-1}$ ) and tracheotomized. A rodent ventilator supplied a mixture of 5%  $\text{CO}_2$ –95% air during the experiments. The tidal volume, respiratory rate, and end-expiratory pressure were 3 mL, 60 breaths/min, and 1 cm  $\text{H}_2\text{O}$ , respectively. A vertical cut was performed near the midline of the thorax and abdomen. Then, heparin (1 U  $\text{g}^{-1}$ ) was injected into the right ventricle. An afferent tube was inserted into the pulmonary artery, and an effluent cannula was inserted into the left atrium through the left ventricle to collect the effluent perfusate. The perfusate was circulated at 8–10 mL/min using a roller pump. The isolated lung remaining *in situ* was placed on an electronic balance. Both the pulmonary arterial pressure (PAP) and the pulmonary venous pressure (PVP, *i.e.*, the left atrial pressure) were measured from the side-arms of the inflow and outflow cannulas.

### Microvascular Permeability

Microvascular permeability ( $K_f$ ) was determined from the increase in lung weight induced by PVP elevation. During the experiment, the PVP rose quickly by 10 cm  $\text{H}_2\text{O}$  and held at this level for at least 7 min. The slow phase of the weight gain was plotted on a semi-logarithmic graph as a function of time ( $\Delta W/\Delta T$ , where  $\Delta W$  is weight gain, and  $\Delta T$  is the length of time). The slow component was then extrapolated to time zero, to estimate the initial capillary filtration rate. The  $K_f$  was defined as the initial weight gain rate (in  $\text{g min}^{-1}$ ) divided by the PVP (10 cm  $\text{H}_2\text{O}$ ) and lung weight, and expressed as grams per minute per centimeter  $\text{H}_2\text{O}^{-1} \times 100$  g [12, 13].

### Determination of LW/BW and W/D Weight Ratios

At the end of the experiments, the rat lung was removed from the hilar region, and the wet weight was obtained for the calculation of the lung weight/body weight

(LW/BW) ratio. To determine the wet/dry (W/D) weight ratio, a part of the lung lobe was dried in a 60 °C incubator for 48 h and weighed.

### Lavage Protein and Cytokine Measurements

After the experiment, the bronchoalveolar lavage fluid (BALF) was obtained by lavaging the left lung twice with 2.5 mL of saline, and the fluid was centrifuged at  $200 \times g$  for 10 min. The protein concentration in the supernatant was determined using a bicinchoninic acid (BCA) protein assay kit (Pierce, Rockford, IL, USA). The levels of tumor necrosis factor (TNF)- $\alpha$  and interleukin-6 (IL-6) in the BALF were measured using a commercial ELISA kit (R&D Systems Inc., Minneapolis, MN, USA).

### Western Blot

Cytoplasmic and nuclear protein extracts were fractionated on 10–12% sodium dodecyl sulfate polyacrylamide gels and immunoblotted with anti-NF- $\kappa$ B p65 (1:1000; Cell Signaling Technology, Danvers, MA, USA), anti-I $\kappa$ B- $\alpha$  (1:1000; Cell Signaling Technology), anti-proliferating cell nuclear antigen (PCNA, 1:2000; Abcam), and anti- $\beta$ -actin antibodies (1:10,000, Sigma-Aldrich) as previously described [13, 14].

### Lung Histological and Neutrophil Count Analyses

The rat lung tissues were stained with hematoxylin and eosin for histologic evaluation. The number of polymorphonuclear neutrophils in the lung interstitium was determined by counting the number of polymorphonuclear neutrophils per high power field ( $\times 400$ ). Two pathologists randomly examined a minimum of 10 fields in a blinded manner and then averaged the counts. Within each field, the lung injury was graded using a lung injury score. Infiltration or aggregation of neutrophils in the airspace or vessel wall and thickness of the alveolar wall were scored according to the following scale: 0, 1, 2, or 3, for no, mild, moderate, or severe injury, respectively. The resulting two scores were added together for the lung injury score [13].

### Experimental Protocols

A total of 30 rats were randomly assigned to the following groups: control, IR, IR + DMEM, IR + NCSC-CM, and IR + heated NCSC-CM. Each group consisted of six rats. In the IR group, the lungs were subjected to 30-min ischemia by stopping ventilation and perfusion. The lungs were then reperfused and ventilated for 90 min after

the ischemia. A 250  $\mu$ L aliquot of concentrated NCSC-CM or DMEM was injected into the perfusate *via* the reservoir 10 min before the ischemia and again after the reperfusion. For the heated NCSC-CM group, the NCSC-CM was heated to 95 °C for 15 min prior to use.

### Statistical Analysis

The data are expressed as mean  $\pm$  SD. Comparison between groups was performed using one-way or two-way repeated measures ANOVA, followed by a *post hoc* comparison using the Bonferroni test. Differences were considered significant at  $P < 0.05$ .

## RESULTS

### Characterization of rat NCSCs

Immunofluorescence analysis of the hair follicle stem cells revealed the expression of SOX10, Snail 1, and p75, which were markers of NCSCs (Fig. 1).

### Effect of NCSC-CM on PAP

In the control group, almost no change in the PAP was observed during the 90-min reperfusion period. Compared to the control and baseline groups, the PAP significantly increased at 90 min in the IR group after reperfusion. The NCSC-CM treatment significantly mitigated the increase in PAP ( $P < 0.05$ ; Fig. 2); however, this protective effect was lost when NCSC-CM was heat-inactivated prior to treatment.

### Effect of NCSC-CM on Vascular Hyperpermeability-Induced by IR

IR-induced significant lung edema, as indicated by the marked increases observed in lung weight (Fig. 3). The increased lung weight was attenuated by NCSC-CM treatment, but not by the heated NCSC-CM treatment. Consistent with these changes, the  $K_f$ , LW/BW, and W/D weight ratios and the lavage protein levels significantly increased in the IR group ( $P < 0.05$ , Fig. 4). Compared to the heated NCSC-CM, NCSC-CM treatment significantly attenuated the increase observed in these variables.

### Effect of NCSC-CM on TNF- $\alpha$ and IL-6 Levels in BALF

Compared to the control group, TNF- $\alpha$  and IL-6 levels in the BALF were significantly higher in the IR

group compared to that of the control group (Fig. 5). Treatment with NCSC-CM significantly reduced this increase, but the heated NCSC-CM did not (Fig. 5).

### Effect of NCSC-CM in Lung Histology

Histological assessment of lung injury was performed using a semiquantitative histopathology score. This analysis revealed that compared to the control group, the IR groups had increased septal thickening and inflammatory cell infiltration (Fig. 6a). Treatment with NCSC-CM significantly attenuated the neutrophil infiltration (Fig. 6b) and lung injury scores, but the heated NCSC-CM did neither (Fig. 6c).

### Effect of NCSC-CM on the NF- $\kappa$ B Signaling Pathway

Nuclear levels of NF- $\kappa$ B p65 significantly increased after IR injury (Fig. 7a); however, compared to the control group, cytoplasmic levels of I $\kappa$ B- $\alpha$  significantly decreased in the IR group (Fig. 7b). Treatment with NCSC-CM restored the decreased I $\kappa$ B- $\alpha$  levels and reduced the elevated nuclear NF- $\kappa$ B p65 levels, but the heated NCSC-CM did neither.

## DISCUSSION

Our study revealed that ALI was induced by 30-min ischemia followed by 90-min reperfusion. Compared to the IR group, NCSC-CM administered before ischemia and after reperfusion reduced pulmonary edema, the degree of histologic lung injury, and the influx of neutrophils into the injured pulmonary alveoli. We also observed a significant decrease in the level of pro-inflammatory cytokines TNF- $\alpha$  and IL-6 in the BALF following NCSC-CM treatment. Additionally, NCSC-CM also reduced I $\kappa$ B- $\alpha$  degradation and the nuclear translocation of NF- $\kappa$ B. However, these protective effects were not observed when heated NCSC-CM was used.

Recent experiments have demonstrated that MSC-CM has protective effects in various animal disease models [6]. MSC-CM reduced the inflammatory response in both IR and D-galactosamine-induced acute liver injury and prolonged the survival in rats with fulminant hepatic failure [6, 14]. Similar protective effects were observed in other models including spinal cord injury, myocardial infarction, and wound healing [15–17]. Moreover, MSC-CM attenuated endotoxin-induced lung injury in mice and *ex vivo* perfused human lungs, as well as neonatal oxygen-induced lung injury [5, 9, 18]. Our study demonstrates for the first

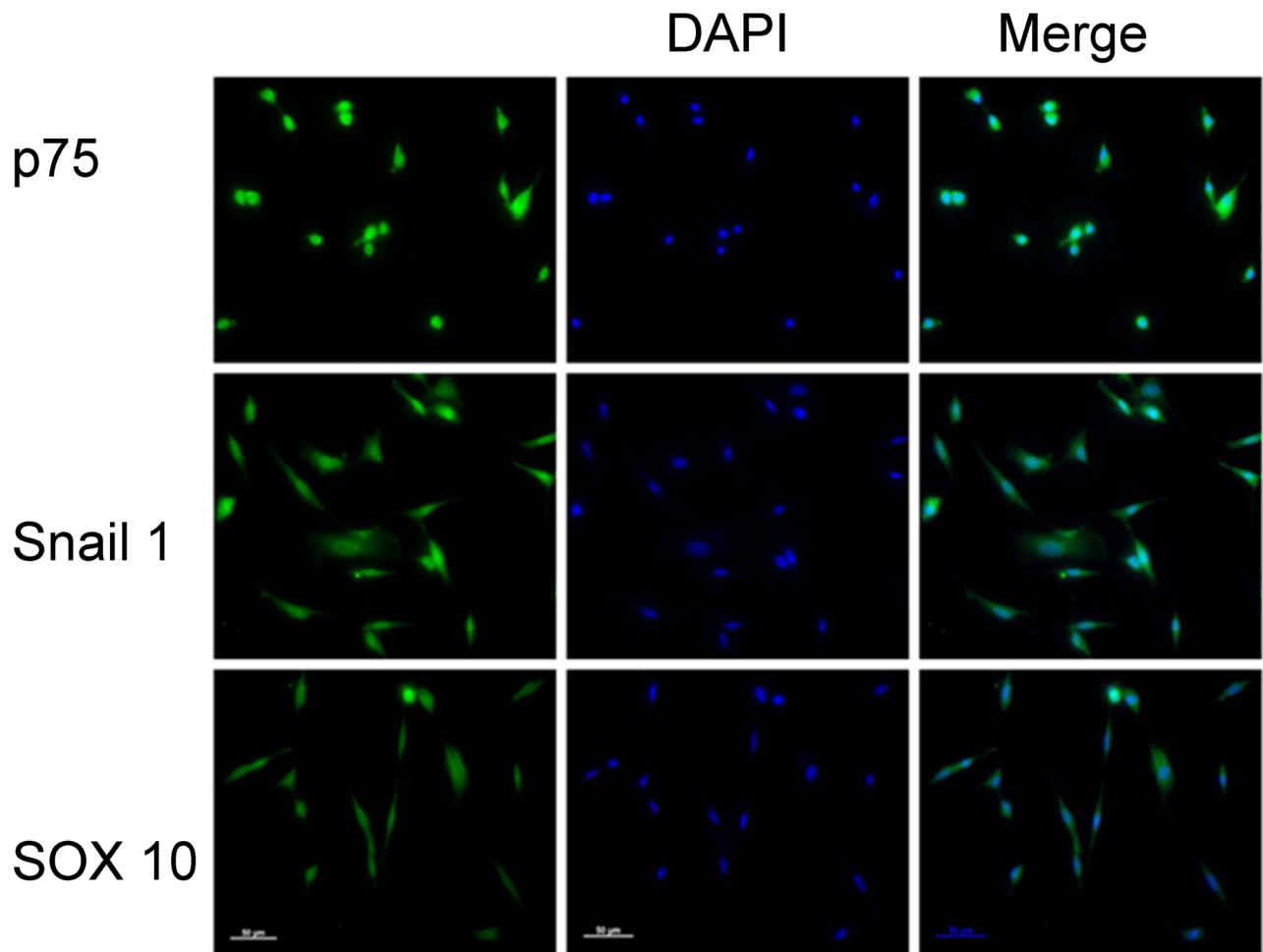


**Fig. 1.** Hair follicle cells express the NCSC markers, Snail 1, p75, and SOX10. Immunofluorescence image analysis revealed that NCSCs expressed p75, Snail 1 and SOX10. Nuclei were counterstained with DAPI (blue). A representative image from one of the three experiments is presented. Bar = 50  $\mu$ m.

time that CM derived from NCSCs attenuated IR-induced ALI.

In the present study, the therapeutic benefit observed following NCSC-CM was in agreement with previous studies using whole cell therapy in IR-induced lung injury [19–21]. Compared with control CM, MSC-CM treatment decreased lung neutrophil influx and pulmonary vascular permeability and improved the lung histopathology. These findings open new therapeutic options for treating IR-induced lung injury. Although the underlying mechanisms regarding the protective effect of NCSC-CM remain unknown, a proteomic analysis of MSC-CM has revealed a broad spectrum of immunomodulatory molecules [6]. Therefore, most investigators have suggested that the wide array of secreted immunomodulatory and growth factors in MSC-CM is responsible for the protective effects [22].

However, the protective effect of NCSC-CM on lung IR injury was eliminated with heat treatment, indicating that heat-labile proteins served as the functional element.

The integrity of the lung microvascular endothelium is important in blocking the influx of fluid with high protein content from plasma as well as inflammatory cells, which may further hinder the ability of the lung epithelium to lessen lung edema [1]. Therefore, NCSC-CM may have beneficial therapeutic effects on the injured lung endothelium. Several soluble paracrine factors, such as angiopoietin-1, keratinocyte growth factor, fibroblast growth factors, and hepatocyte growth factor, were found to maintain the integrity of pulmonary endothelial cells, restore lung endothelial and epithelial permeability, improve the ability of the alveolar epithelium to remove alveolar edema fluid, and inhibit leukocyte–endothelium



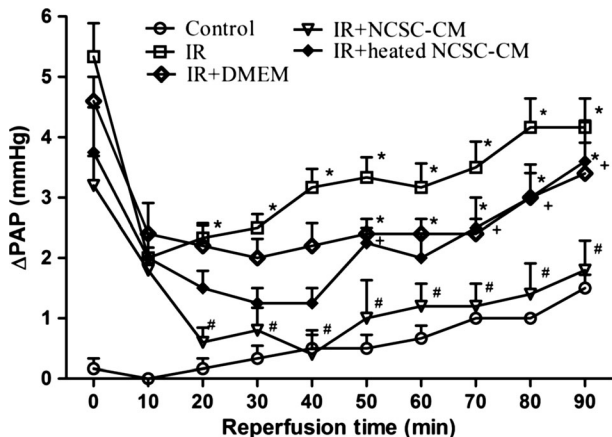


**Fig. 2.** Effect of NCSC-CM on pulmonary artery pressure ( $\Delta$ PAP). PAP significantly increased in the ischemia-reperfusion (IR) group. The increase in PAP was significantly attenuated by treatment with NCSC-CM but not by treatment with heated NCSC-CM. Data are expressed as mean  $\pm$  SD ( $n = 6$  per group). \* $P < 0.05$ , compared to the control group; # $P < 0.05$ , compared to the IR group; + $P < 0.05$ , compared to the IR+NCSC-CM group.

interactions by modifying endothelial cell adhesion molecules and cell junctions [18, 23, 24]. In the present study, NCSC-CM attenuated pulmonary edema, as indicated by the reduced  $K_f$ , the low W/D and LW/BW ratios, and the decreased protein concentration in the BALF. Our results are in agreement with those of other groups. In the future, it

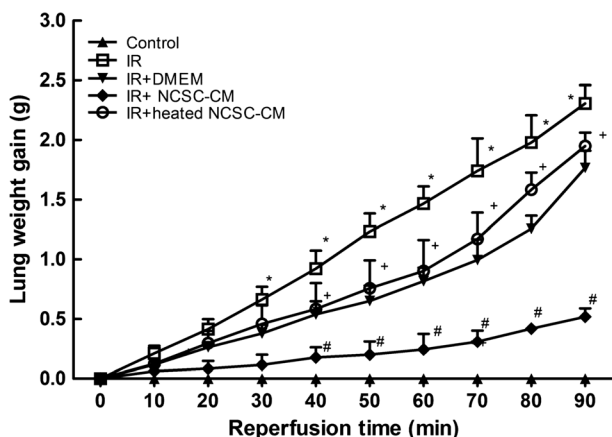


**Fig. 3.** Effect of NCSC-CM on the lung weight gain, ischemia-reperfusion (IR) led to significant lung weight gain (LWG). The increase in the LWG was significantly attenuated by NCSC-CM treatment, but not by heated NCSC-CM treatment. All data are shown as mean  $\pm$  SD ( $n = 6$  per group). \* $P < 0.05$ , compared to the control group; # $P < 0.05$ , compared to the IR group; + $P < 0.05$ , compared to the IR+NCSC-CM group.

will be important to recognize the contribution of each soluble factor in NCSC-CM to lung endothelial permeability in ALI.

MSC soluble paracrine factors have anti-inflammatory and immunomodulatory effects. These soluble factors include indoleamine 2, 3-dioxygenase, IL-10, TNF-stimulated gene 6, prostaglandin E2, IL-1 receptor antagonist, transforming growth factor (TGF)- $\beta$ , and hepatocyte growth factor [6]. The downregulation of pro-inflammatory mediators (IL-1 $\beta$ , TNF- $\alpha$ , and IL-6) and the upregulation of anti-inflammatory cytokines (IL-10, TGF- $\alpha$ , and TGF- $\beta$ ) have been shown to be the major factors in treating diseases, such as acute kidney and liver injury, acute stroke, and sepsis [2]. In these disease models, MSCs reduced the levels of TNF- $\alpha$  in the BALF and plasma, which blocked the influx of polymorphonuclear neutrophils into the injured tissue and prevented further damage [2]. Our study demonstrated that NCSC-CM decreased the expression of TNF- $\alpha$  and IL-6 in the BALF and neutrophil infiltration in lung tissue, similar to these previous reports.

IL-6 is mostly regarded as a pro-inflammatory cytokine for perpetuating chronic inflammation and autoimmunity. IL-6 also coordinates the anti-inflammatory activities essential for the resolution of inflammation [25]; however, these effects are context dependent [25]. Investigations showed that IL-6 limited influenza virus-induced inflammation and protected against hyperoxic acute lung injury in animal models [26, 27]. Further, Zhang et al. demonstrated that the therapeutic effects of adipose-derived stem cells (ASCs) in LPS-induced ALI were IL-6 mediated [28]. In contrast in ARDS patients, higher IL-6 levels in plasma and BALF were associated with poor outcomes [29]. Dental pulp-derived stem cell CM also reduced cardiac IL-6 mRNA levels following IR cardiac injury [30]. Further, ASC-CM decreased IL-6 production in air pouch exudates in the zymosan-induced mouse air pouch model and serum IL-6 levels in hepatic ischemia-reperfusion injury [31, 32]. These findings are comparable with our results.

The transcription factor, NF- $\kappa$ B, regulates and enhances the expression of inflammatory mediators and adhesion molecules, resulting in the recruitment of a large influx of inflammatory cells to the lung. NF- $\kappa$ B activation involves the phosphorylation and subsequent degradation of I $\kappa$ B- $\alpha$ , which allows NF- $\kappa$ B to translocate to the nucleus and initiate the transcription of inflammatory genes such as TNF- $\alpha$  and IL-6 [33, 34]. Previous and current studies have revealed that IR-induced lung injury decreases I $\kappa$ B- $\alpha$  levels and induces NF- $\kappa$ B signaling activation. The activation of the NF- $\kappa$ B signaling pathway triggered the

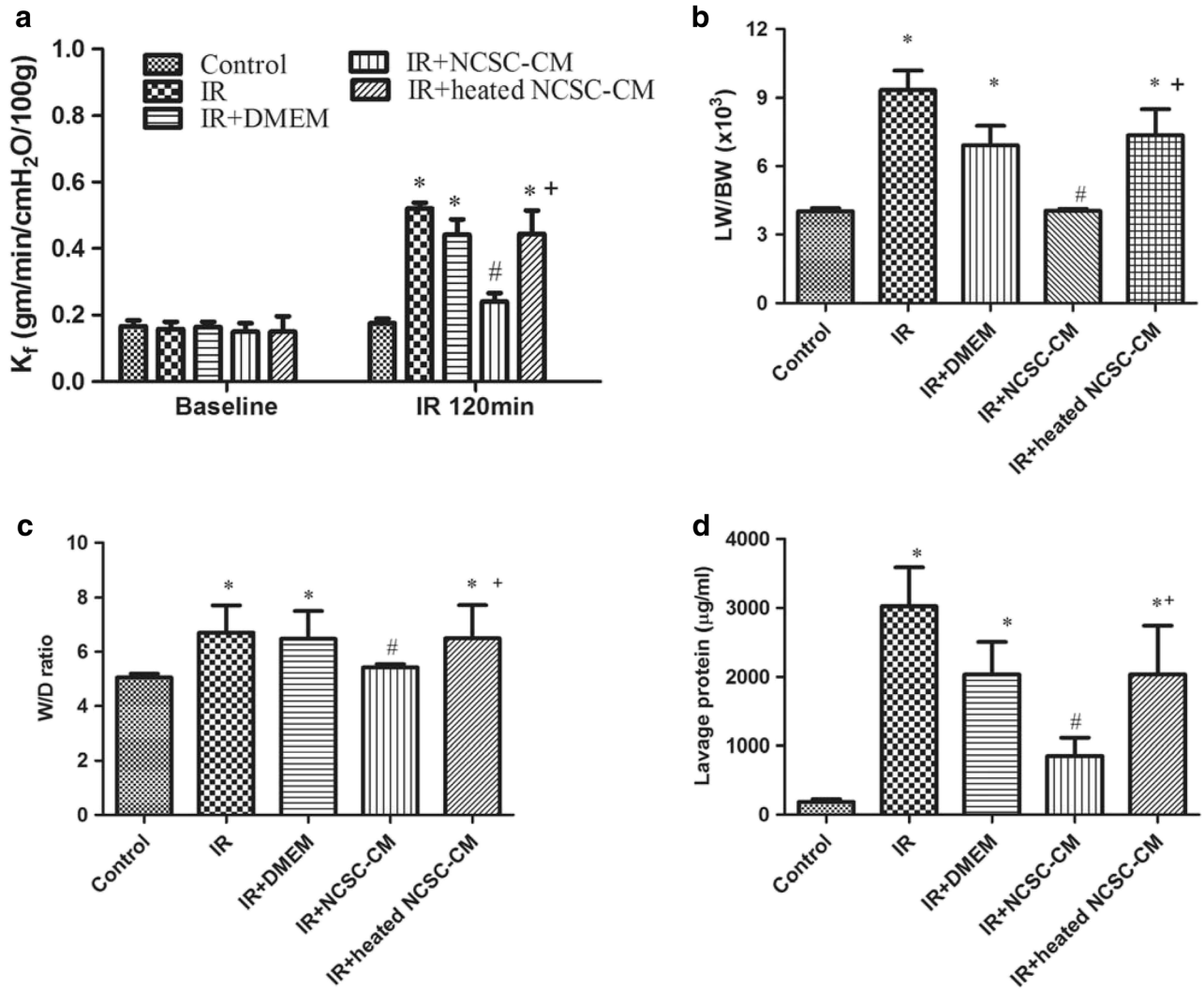


**Fig. 4.** Effect of NCSC-CM on the indicators of lung edema. Ischemia-reperfusion (IR) significantly increased the  $K_f$  (a), the lung weight/body weight (LW/BW) ratio (b), the wet/dry (W/D) weight ratio (c), and the protein concentration in bronchoalveolar lavage (BALF) (d). The increases in these indicators were significantly attenuated by NCSC-CM treatment, but not by heated NCSC-CM treatment. All data are shown as mean  $\pm$  SD ( $n = 6$  per group). \* $P < 0.05$ , compared to the control group; # $P < 0.05$ , compared to the IR group; + $P < 0.05$ , compared to the IR+ NCSC-CM group.

production and secretion of cytokines and chemokines [10–13]. In this study, we showed that NCSC-CM suppressed the NF- $\kappa$ B signaling pathway in IR lung injury by inhibiting the degradation of I $\kappa$ B- $\alpha$  and the nuclear translocation of NF- $\kappa$ B. Consequently, NCSC-CM reduced the production of TNF- $\alpha$  and IL-6 after IR injury to the lung. These results were similar to those of previous experiments showing that MSCs suppressed NF- $\kappa$ B activation in reporter cells following incubation with LPS-inflamed serum and in IR lung injury in rats [35, 36].

Although the protective effects of NCSC-CM could be attributed primarily to the release of paracrine factors, a proteomic analysis of CM will be necessary to determine whether other factors are also critical in treating ALI and ARDS. A variety of other factors may be present in CM and act in combination to elicit the observed protection. Therefore, it is important to analyze a complete set of growth factor and cytokine levels from different stem cell-derived CM. The optimal culture condition, CM processing, dose, and route,

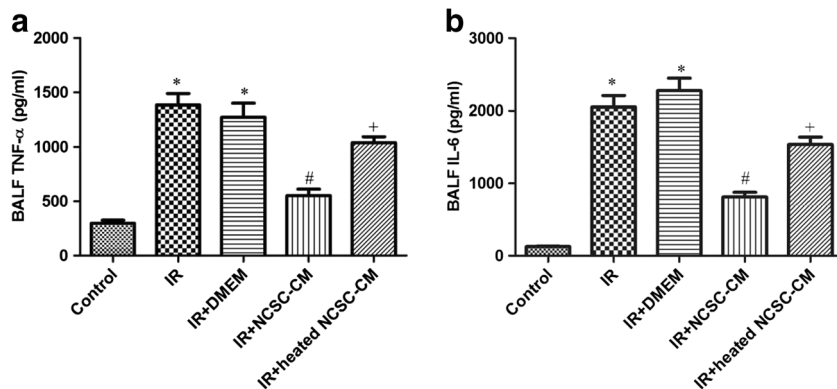


**Fig. 5.** Effect of NCSC-CM on TNF- $\alpha$  and IL-6 levels in bronchoalveolar lavage fluid (BALF). Ischemia-reperfusion (IR) significantly increased TNF- $\alpha$  and IL-6 levels in BALF. The increase was significantly suppressed by NCSC-CM treatment, but not by heated NCSC-CM treatment. All data are shown as mean  $\pm$  SD ( $n = 6$  per group). \* $P < 0.05$ , compared to the control group; # $P < 0.05$ , compared to the IR group; + $P < 0.05$ , compared to the IR+ NCSC-CM group.

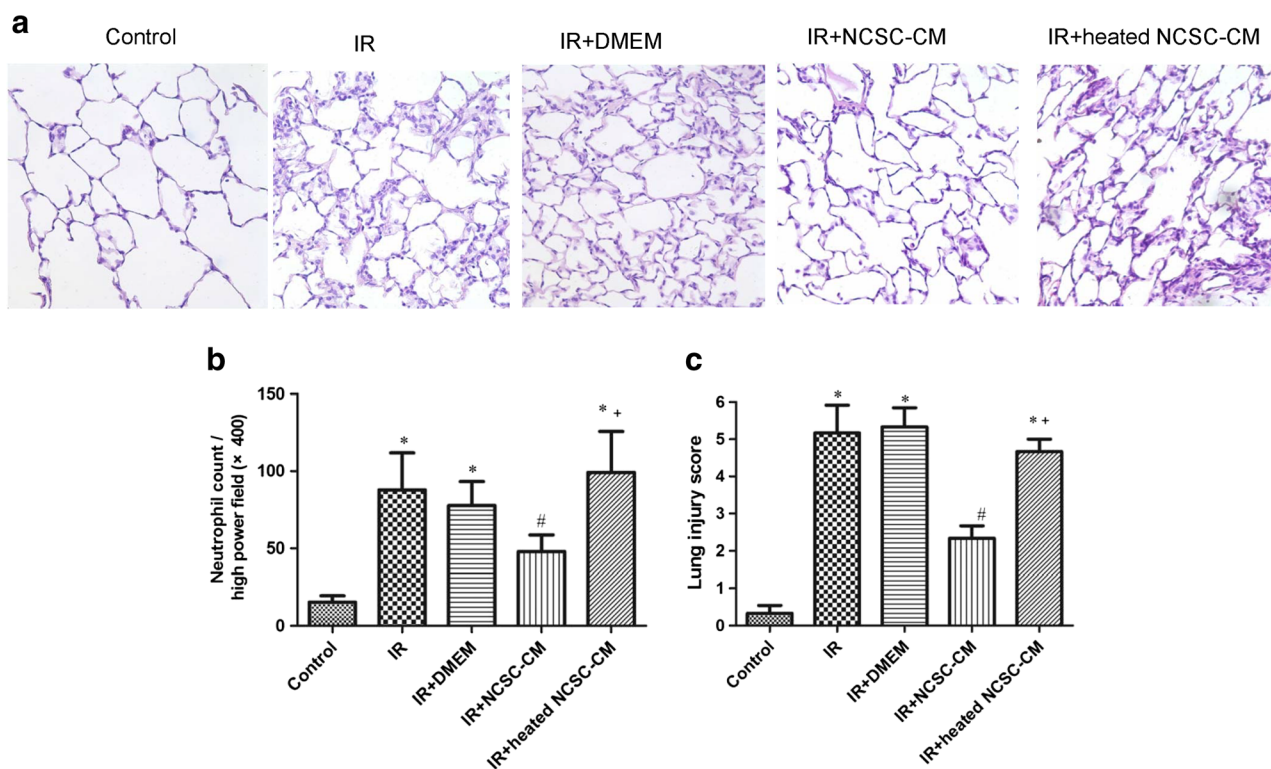


**Fig. 6.** Effect of NCSC-CM on lung histopathology. Compared to a representative section of lung tissue ( $\times 400$  magnification), tissues exposed to ischemia-reperfusion (IR) had a significantly increased number of infiltrating neutrophils and septal thickness (a). NCSC-CM treatment, but not heated NCSC-CM treatment, improved the histological changes. Lung injury scores (b) and the numbers of neutrophils per high power field ( $\times 400$  magnification) (c) were significantly greater in the IR group than in the control group. These increases were significantly attenuated by NCSC-CM treatment but not by heated NCSC-CM treatment. All data are shown as mean  $\pm$  SD ( $n = 6$  per group). \* $P < 0.05$ , compared to the control group; # $P < 0.05$ , compared with the IR group; + $P < 0.05$ , compared to the IR+ NCSC-CM group.



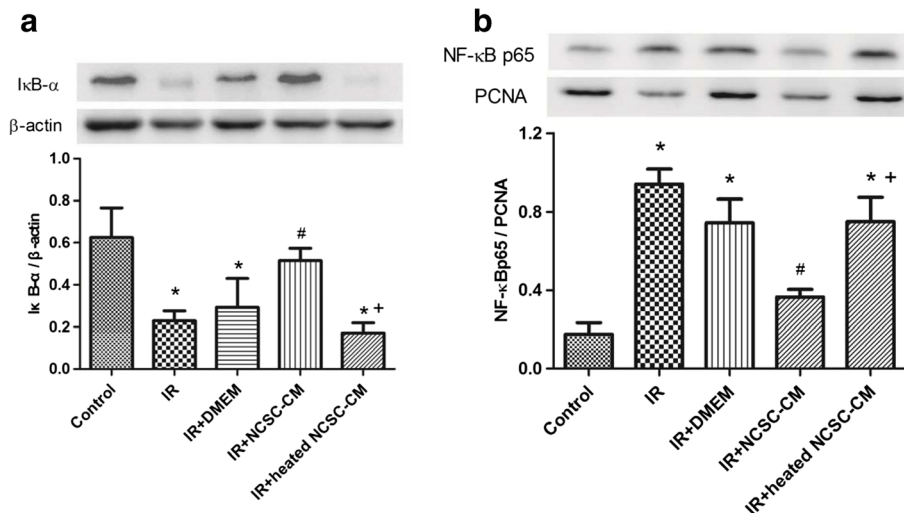


**Fig. 7.** Effect of NCSC-CM on the expression of nuclear NF- $\kappa$ B p65 and cytoplasmic I $\kappa$ B- $\beta$  in the lung tissues. Treatment with NCSC-CM, but not heated NCSC-CM, increased I $\kappa$ B- $\beta$  levels (a) and reduced nuclear NF- $\kappa$ B p65 levels (b) in ischemia-reperfusion (IR)-induced lung injury. PCNA and  $\beta$ -actin served as loading controls for nuclear and cytoplasmic proteins, respectively. A representative blot is shown. Data are expressed as mean  $\pm$  SD ( $n = 3$  per group). \* $P < 0.05$ , compared to the control group; # $P < 0.05$ , compared to the IR group; + $P < 0.05$ , compared to the IR+ NCSC-CM group.

as well as the diseases that are responsive to CM therapy, need to be further investigated [22]. Recent *in vivo* studies underscore the potential new role of microvesicles or exosomes released from MSCs as a paracrine vehicle to deliver messenger RNA or proteins to targeted cells and affect multiple biological events [37, 38].

In this study, we demonstrated that NCSC-CM significantly restored alveolar-capillary integrity, as observed in decreased pulmonary edema and improvements in lung tissue damage. NCSC-CM attenuated the increased inflammatory response, I $\kappa$ B- $\alpha$  degradation, and nuclear translocation of NF- $\kappa$ B in lung tissue injuries induced by IR. These results imply that NCSC-CM may be a therapeutic option in IR-induced lung injury. Because multipotent NCSCs in hair follicle bulges are relatively easy to harvest and culture in the laboratory, this investigation may lead to new approaches in the use of NCSC-CM to treat IR-induced lung injury.

#### ACKNOWLEDGMENTS

The study was supported, in part, by grants NSC 100-2314-B-016-038 and MOST 103-2314-B-016-029-MY3 from the Ministry of Science and Technology, grants TSGH-C104-067, TSGH-C101-086, and TSGH-C99-057 from the Tri-Service General Hospital, grant 10301 from

the Taoyuan Armed Forces General Hospital, and grants MAB-104-052, MAB102-050, and CH-NDMC-105-2 from the National Defense Medical Center, Taipei, Taiwan.

#### REFERENCES

- Matthay, M.A., and G.A. Zimmerman. 2005. Acute lung injury and the acute respiratory distress syndrome: four decades of inquiry into pathogenesis and rational management. *American Journal of Respiratory Cell and Molecular Biology* 33: 319–327.
- Monsel, A., Y.G. Zhu, S. Gennai, Q. Hao, J. Liu, and J.W. Lee. 2014. Cell-based therapy for acute organ injury: preclinical evidence and ongoing clinical trials using mesenchymal stem cells. *Anesthesiology* 121: 1099–1121.
- Wang, Y.Y., X.Z. Li, and L.B. Wang. 2013. Therapeutic implications of mesenchymal stem cells in acute lung injury/acute respiratory distress syndrome. *Stem Cell Research & Therapy* 4: 45.
- Curley, G.F., B. Ansari, M. Hayes, J. Devaney, C. Masterson, A. Ryan, F. Barry, T. O'Brien, D.O. Toole, and J.G. Laffey. 2013. Effects of intratracheal mesenchymal stromal cell therapy during recovery and resolution after ventilator-induced lung injury. *Anesthesiology* 118: 924–932.
- Aslam, M., R. Baveja, O.D. Liang, A. Fernandez-Gonzalez, C. Lee, S.A. Mitsialis, and S. Kourembanas. 2009. Bone marrow stromal cells attenuate lung injury in a murine model of neonatal chronic lung disease. *American Journal of Respiratory and Critical Care Medicine* 180: 1122–1130.

6. Makridakis, M., M.G. Roubelakis, and A. Vlahou. 2013. Stem cells: insights into the secretome. *Biochimica et Biophysica Acta* 1834: 2380–2384.
7. Sieber-Blum, M. 2014. Human epidermal neural crest stem cells as candidates for cell-based therapies, disease modeling, and drug discovery. *Birth Defects Research. Part C, Embryo Today* 102: 221–226.
8. Sieber-Blum, M., M. Grim, Y.F. Hu, and V. Szeder. 2004. Pluripotent neural crest stem cells in the adult hair follicle. *Developmental Dynamics* 231: 258–269.
9. Ionescu, L., R.N. Byrne, T. van Haften, A. Vadivel, R.S. Alphonse, G.J. Rey-Parra, G. Weissmann, A. Hall, F. Eaton, and B. Thebaud. 2012. Stem cell conditioned medium improves acute lung injury in mice: in vivo evidence for stem cell paracrine action. *American Journal of Physiology. Lung Cellular and Molecular Physiology* 303: L967–L977.
10. Peng, C.K., K.L. Huang, C.P. Wu, M.H. Li, Y.T. Hu, C.W. Hsu, S.H. Tsai, and S.J. Chu. 2011. Glutamine protects ischemia-reperfusion induced acute lung injury in isolated rat lungs. *Pulmonary Pharmacology & Therapeutics* 24: 153–161.
11. Wu, S.Y., S.E. Tang, F.C. Ko, G.C. Wu, K.L. Huang, and S.J. Chu. 2015. Valproic acid attenuates acute lung injury induced by ischemia-reperfusion in rats. *Anesthesiology* 122: 1327–1337.
12. Wu, S.Y., M.H. Li, F.C. Ko, G.C. Wu, K.L. Huang, and S.J. Chu. 2013. Protective effect of hypercapnic acidosis in ischemia-reperfusion lung injury is attributable to upregulation of heme oxygenase-1. *PLoS One* 8: e74742.
13. Wu, S.Y., C.P. Wu, B.H. Kang, M.H. Li, S.J. Chu, and K.L. Huang. 2012. Hypercapnic acidosis attenuates reperfusion injury in isolated and perfused rat lungs. *Critical Care Medicine* 40: 553–559.
14. Parekkadan, B., D. van Poll, K. Suganuma, E.A. Carter, F. Berthiaume, A.W. Tilles, and M.L. Yarmush. 2007. Mesenchymal stem cell-derived molecules reverse fulminant hepatic failure. *PLoS One* 2: e941.
15. Cantinieaux, D., R. Quertainmont, S. Blacher, L. Rossi, T. Wanet, A. Noel, G. Brook, J. Schoenen, and R. Franzen. 2013. Conditioned medium from bone marrow-derived mesenchymal stem cells improves recovery after spinal cord injury in rats: an original strategy to avoid cell transplantation. *PLoS One* 8: e69515.
16. Gneccchi, M., H. He, N. Noiseux, O.D. Liang, L. Zhang, F. Morello, H. Mu, L.G. Melo, R.E. Pratt, J.S. Ingwall, and V.J. Dzau. 2006. Evidence supporting paracrine hypothesis for Akt-modified mesenchymal stem cell-mediated cardiac protection and functional improvement. *The FASEB Journal* 20: 661–669.
17. Walter, M.N., K.T. Wright, H.R. Fuller, S. MacNeil, and W.E. Johnson. 2010. Mesenchymal stem cell-conditioned medium accelerates skin wound healing: an in vitro study of fibroblast and keratinocyte scratch assays. *Experimental Cell Research* 316: 1271–1281.
18. Lee, J.W., X. Fang, N. Gupta, V. Serikov, and M.A. Matthay. 2009. Allogeneic human mesenchymal stem cells for treatment of *E. coli* endotoxin-induced acute lung injury in the ex vivo perfused human lung. *Proceedings of the National Academy of Sciences of the United States of America* 106: 16357–16362.
19. Sun, C.K., C.H. Yen, Y.C. Lin, T.H. Tsai, L.T. Chang, Y.H. Kao, S. Chua, M. Fu, S.F. Ko, S. Leu, and H.K. Yip. 2011. Autologous transplantation of adipose-derived mesenchymal stem cells markedly reduced acute ischemia-reperfusion lung injury in a rodent model. *Journal of Translational Medicine* 9: 118.
20. Chen, S., L. Chen, X. Wu, J. Lin, J. Fang, X. Chen, S. Wei, J. Xu, Q. Gao, and M. Kang. 2012. Ischemia postconditioning and mesenchymal stem cells engraftment synergistically attenuate ischemia reperfusion-induced lung injury in rats. *The Journal of Surgical Research* 178: 81–91.
21. Manning, E., S. Pham, S. Li, R.I. Vazquez-Padron, J. Mathew, P. Ruiz, and S.K. Salgar. 2010. Interleukin-10 delivery via mesenchymal stem cells: a novel gene therapy approach to prevent lung ischemia-reperfusion injury. *Human Gene Therapy* 21: 713–727.
22. Pawitan, J.A. 2014. Prospect of stem cell conditioned medium in regenerative medicine. *BioMed Research International* 2014: 965849.
23. McCarter, S.D., S.H. Mei, P.F. Lai, Q.W. Zhang, C.H. Parker, R.S. Suen, R.D. Hood, Y.D. Zhao, Y. Deng, R.N. Han, D.J. Dumont, and D.J. Stewart. 2007. Cell-based angiopoietin-1 gene therapy for acute lung injury. *American Journal of Respiratory and Critical Care Medicine* 175: 1014–1026.
24. Lee, J.W., X. Fang, A. Krasnodembskaya, J.P. Howard, and M.A. Matthay. 2011. Concise review: mesenchymal stem cells for acute lung injury: role of paracrine soluble factors. *Stem Cells* 29: 913–919.
25. Hunter, C.A., and S.A. Jones. 2015. IL-6 as a keystone cytokine in health and disease. *Nature Immunology* 16: 448–457.
26. Lauder, S.N., E. Jones, K. Smart, A. Bloom, A.S. Williams, J.P. Hindley, B. Ondondo, P.R. Taylor, M. Clement, C. Fielding, A.J. Godkin, S.A. Jones, and A.M. Gallimore. 2013. Interleukin-6 limits influenza-induced inflammation and protects against fatal lung pathology. *European Journal of Immunology* 43: 2613–2625.
27. Ward, N.S., A.B. Waxman, R.J. Homer, L.L. Mantell, O. Einarsson, Y. Du, and J.A. Elias. 2000. Interleukin-6-induced protection in hyperoxic acute lung injury. *American Journal of Respiratory Cell and Molecular Biology* 22: 535–542.
28. Zhang, S., S.D. Danchuk, R.W. Bonvillain, B. Xu, B.A. Scruggs, A.L. Strong, J.A. Semon, J.M. Gimble, A.M. Betancourt, D.E. Sullivan, and B.A. Bunnell. 2014. Interleukin 6 mediates the therapeutic effects of adipose-derived stromal/stem cells in lipopolysaccharide-induced acute lung injury. *Stem Cells* 32: 1616–1628.
29. Bhargava, M., and C.H. Wendt. 2012. Biomarkers in acute lung injury. *Translational Research* 159: 205–217.
30. Yamaguchi, S., R. Shibata, N. Yamamoto, M. Nishikawa, H. Hibi, T. Tanigawa, M. Ueda, T. Murohara, and A. Yamamoto. 2015. Dental pulp-derived stem cell conditioned medium reduces cardiac injury following ischemia-reperfusion. *Scientific Reports* 5: 16295.
31. Lee, S.C., J.O. Kim, and S.J. Kim. 2015. Secretome from human adipose-derived stem cells protects mouse liver from hepatic ischemia-reperfusion injury. *Surgery* 157: 934–943.
32. Carceller, M.C., M.I. Guillen, M.L. Ferrandiz, and M.J. Alcaraz. 2015. Paracrine in vivo inhibitory effects of adipose tissue-derived mesenchymal stromal cells in the early stages of the acute inflammatory response. *Cytotherapy* 17: 1230–1239.
33. Liu, S.F., and A.B. Malik. 2006. NF-kappa B activation as a pathological mechanism of septic shock and inflammation. *American Journal of Physiology. Lung Cellular and Molecular Physiology* 290: L622–L645.
34. Libermann, T.A., and D. Baltimore. 1990. Activation of interleukin-6 gene expression through the NF-kappa B transcription factor. *Molecular and Cellular Biology* 10: 2327–2334.
35. Yagi, H., A. Soto-Gutierrez, N. Navarro-Alvarez, Y. Nahmias, Y. Goldwasser, Y. Kitagawa, A.W. Tilles, R.G. Tompkins, B. Parekkadan, and M.L. Yarmush. 2010. Reactive bone marrow stromal cells attenuate systemic inflammation via sTNFR1. *Molecular Therapy* 18: 1857–1864.
36. Sun, C.K., S. Leu, S.Y. Hsu, Y.Y. Zhen, L.T. Chang, C.Y. Tsai, Y.L. Chen, Y.T. Chen, T.H. Tsai, F.Y. Lee, J.J. Sheu, H.W. Chang, and H.K. Yip. 2015. Mixed serum-deprived and normal adipose-derived mesenchymal stem cells against acute lung ischemia-reperfusion injury in rats. *American Journal of Translational Research* 7: 209–231.

37. Gennai, S., A. Monsel, Q. Hao, J. Park, M.A. Matthay, and J.W. Lee. 2015. Microvesicles derived from human mesenchymal stem cells restore alveolar fluid clearance in human lungs rejected for transplantation. *American Journal of Transplantation* 15: 2404–2412.
38. Akyurekli, C., Y. Le, R.B. Richardson, D. Fergusson, J. Tay, and D.S. Allan. 2015. A systematic review of preclinical studies on the therapeutic potential of mesenchymal stromal cell-derived microvesicles. *Stem Cell Reviews* 11: 150–160.